Supporting Information for

Enhanced photocatalytic activity of g-C_3N_4/MnO composites for hydrogen evolution under visible light

Na Mao[a,b], Xiaomin Gao[a], Chong Zhang[a], Chang Shu[a], Wenyan Ma[a], Feng Wang[c,d], and Jia-Xing Jiang[a,*]

[a] *Shaanxi Key Laboratory for Advanced Energy Devices, Key Laboratory for Macromolecular Science of Shaanxi Province, School of Materials Science and Engineering, Shaanxi Normal University, Xi'an, Shaanxi, 710062, P. R. China. E-mail: jiaxing@snnu.edu.cn.*

[b] *College of Chemistry and Materials, Weinan Normal University, Weinan 714099, P. R. China*

[c] *Key Laboratory for Green Chemical Process of Ministry of Education, School of Chemical Engineering and Pharmacy, Wuhan Institute of Technology, Wuhan 430073, P. R. China*

[d] *School of Materials Science and Engineering, Zhengzhou University, Zhengzhou 450001, China*

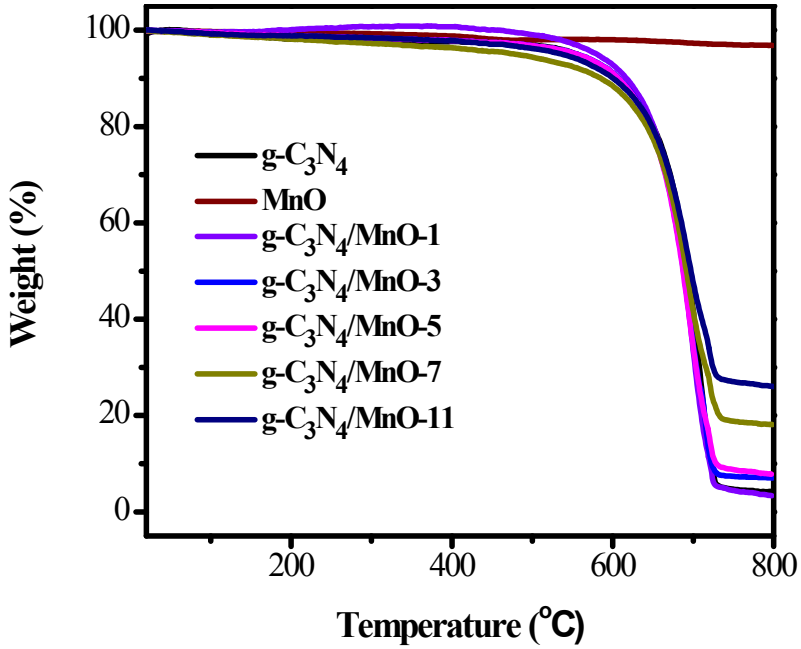

Fig. S1. Thermogravimetric analysis curves of g-C_3N_4 and the g-C_3N_4/MnO composites under N_2 atmosphere.

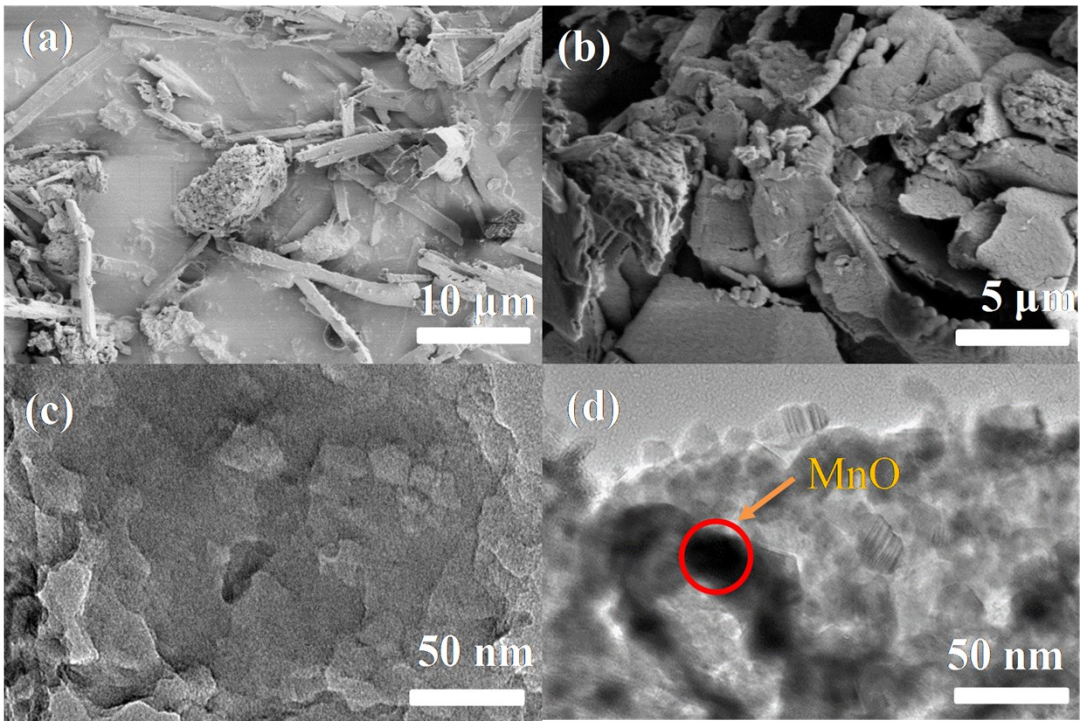

Fig. S2. (a) and (b) Scanning electron microscopy images of pure g-C_3N_4 from melamine, (c) Transmission electron microscopy images of g-C_3N_4 and (d) the g-C_3N_4/MnO-5 composite.

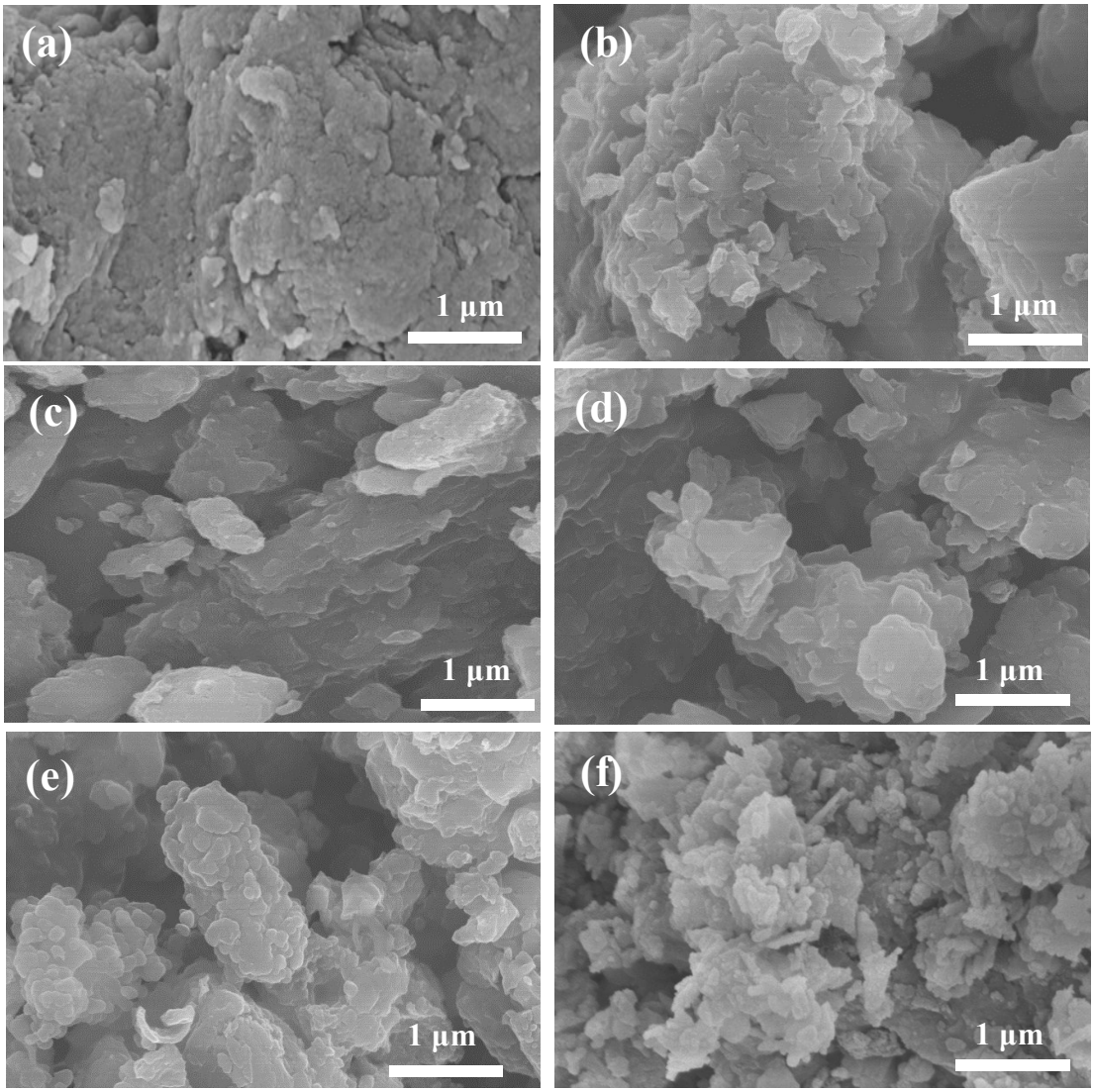

Fig. S3. Scanning electron microscopy images of (a) pure g-C_3N_4; (b) g-C_3N_4/MnO-1 composite; (c) g-C_3N_4/MnO-3 composite; (d) g-C_3N_4/MnO-5 composite; (e) g-C_3N_4/MnO-7 composite; (f) g-C_3N_4/MnO-11 composite;

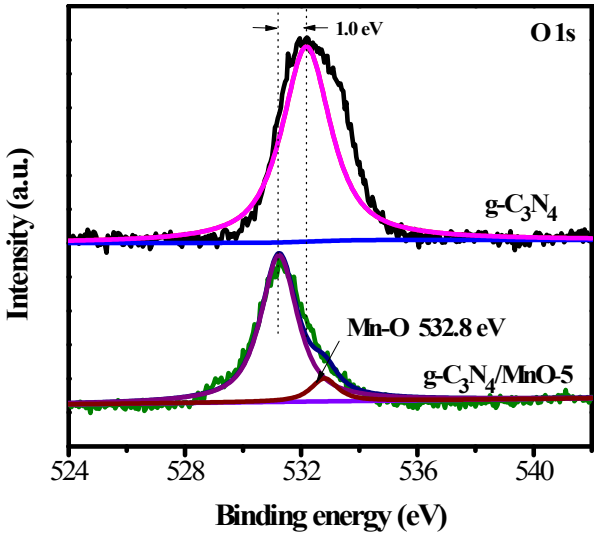

Fig. S4. XPS spectra of the bare g-C_3N_4 and the g-C_3N_4/MnO-5 composite for O 1s.

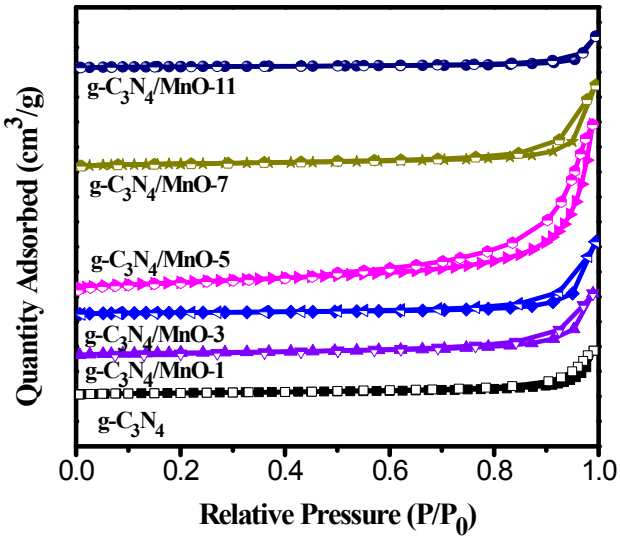

Fig. S5. Nitrogen adsorption (filled symbols) / desorption (empty symbols) isotherms for the bare g-C_3N_4 and the g-C_3N_4/MnO composites collected at 77.3 K.

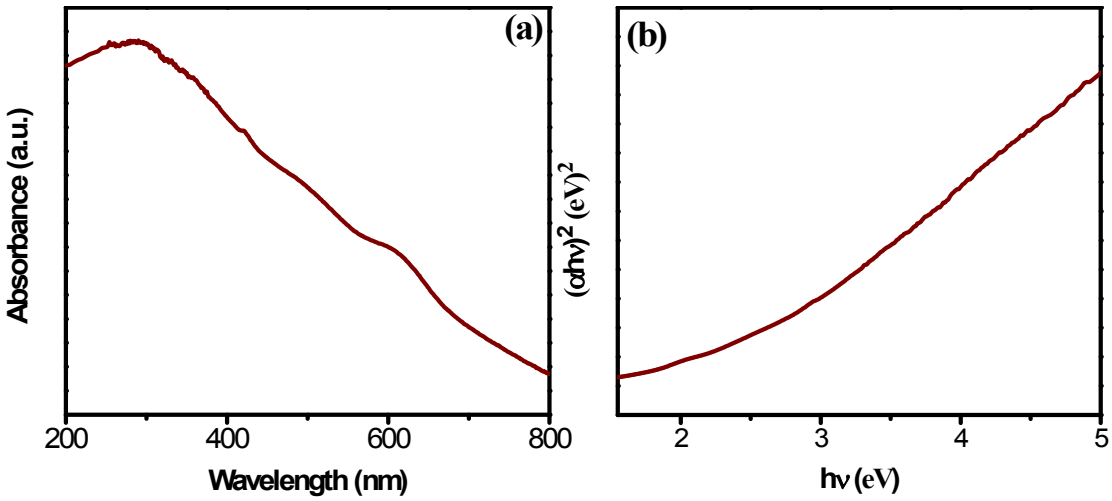

Fig. S6. (a) The UV-Vis reflection spectrum of MnO; (b) Band-gap plot for MnO.

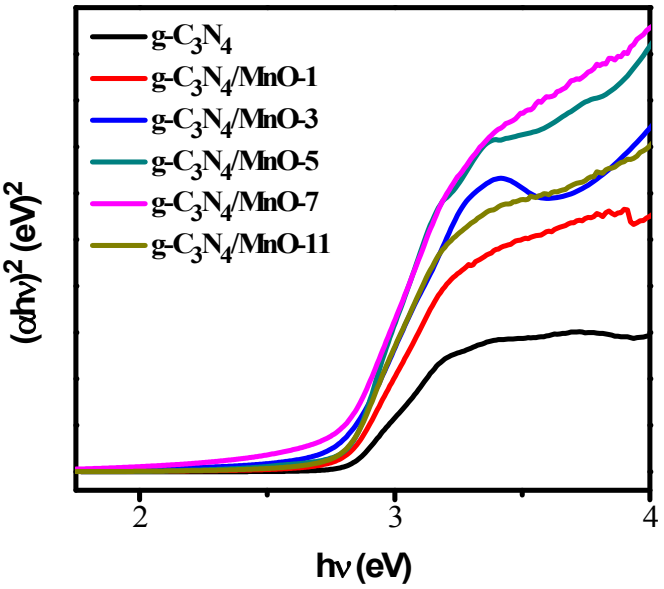

Fig. S7. Band-gap plots of all of the samples.

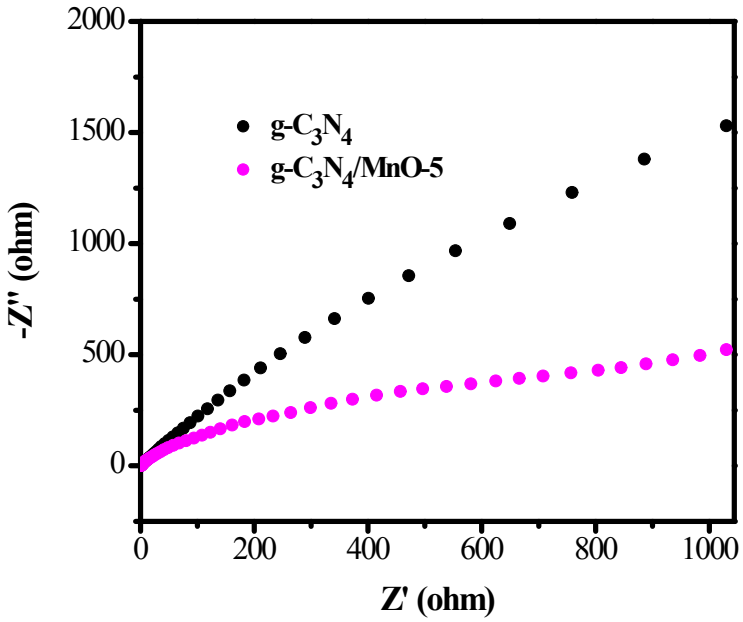

Fig. S8. EIS plots of the bare g-C_3N_4 and the g-C_3N_4/MnO-5 composite.

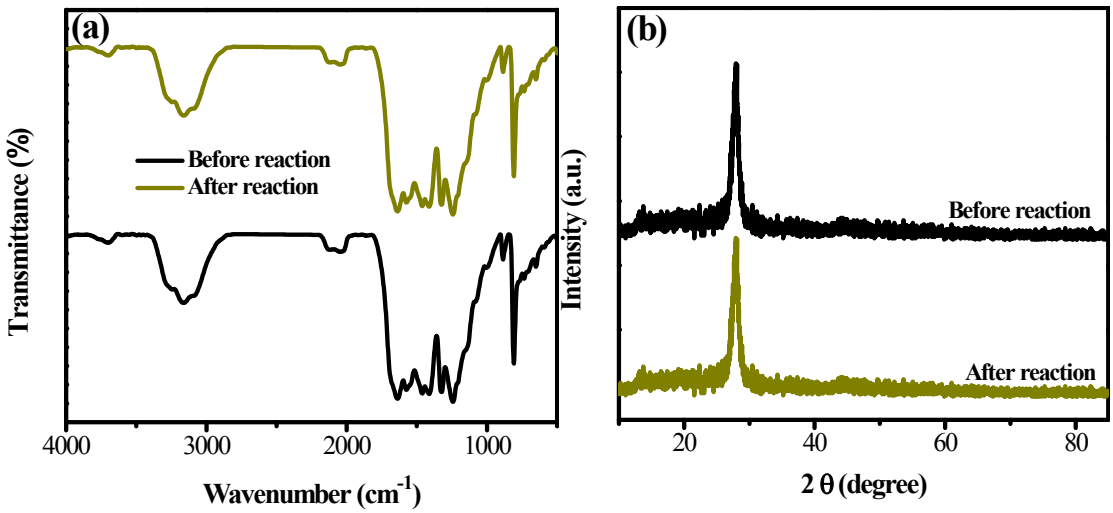

Fig. S9. (a) FT-IR spectra, and (b) Powder XRD patterns of the g-C_3N_4/MnO-5 composite before and after irradiation under visible light (λ >400 nm) for 15 h in a triethanolamine/water mixture.

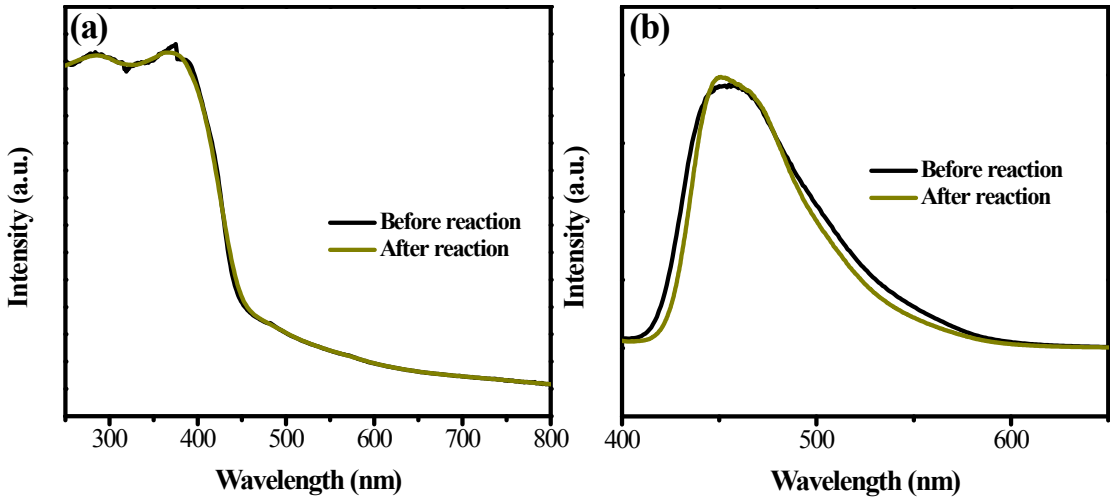

Fig. S10. (a) UV-Vis spectra of the g-C_3N_4/MnO-5 composite, and (b) Photoluminescence spectra ($\lambda_{excitation}$ = 365 nm) of the g-C_3N_4/MnO-5 composite before and after irradiation under visible light (λ >400 nm) for 15 h in a triethanolamine/water mixture.

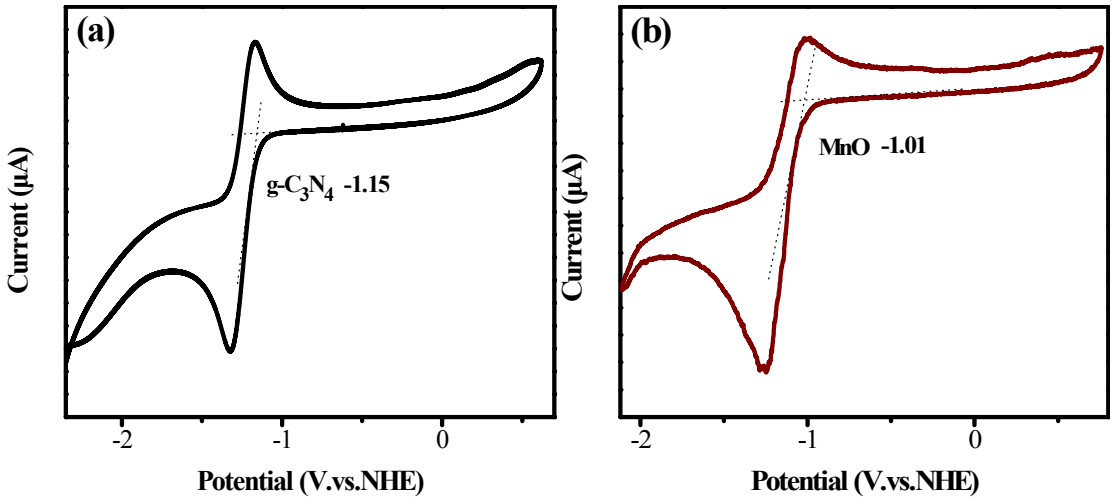

Fig. S11. Cyclic voltammetry measurement for (a) g-C_3N_4 and (b) MnO.

Table S1. Weight percentage of C, N, O, Mn in the g-C_3N_4/MnO-5 composite and g-C_3N_4

samples	Weight (%)			Atomic Ratios	
	C[(a)]	N[(a)]	Mn[(b)]	N/C	C/Mn
g-C_3N_4	34.66	59.25	--	1.54	-
g-C_3N_4/MnO-5	32.51	57.64	2.89	1.56	54

(a) Data obtained by EA, (b) Data obtained by ICP-MS

Table S2. The BET surface area, pore volume and pore size of g-C_3N_4, g-C_3N_4/MnO-5 composite

Photocatalyst	[a]S_{BET} / $m^2 \cdot g^{-1}$	[b]Pore volume/$cm^3 \cdot g^{-1}$	Pore size/nm
g-C_3N_4	12	0.06	20.8
g-C_3N_4/MnO-1	13	0.10	29.4
g-C_3N_4/MnO-3	14	0.01	33.3
g-C_3N_4/MnO-5	48	0.25	18.8
g-C_3N_4/MnO-7	18	0.13	28.8
g-C_3N_4/MnO-11	6	0.03	23.5
MnO	9	0.05	0

a. BET Surface Area; b. *t-plot* micropore volume.

Table S3. Radiative fluorescence lifetimes and their relative percentages of photoexcited charge carriers in the g-$C_3N_4$and g-C_3N_4/MnO-5 composite.

Sample	τ_1(ns)(Rel %)	τ_2(ns)(Rel %)	τ_3(ns)(Rel %)	t_{av}(ns)[a]
g-C_3N_4	1.13-38.00	4.41-47.55	26.62-14.45	17.62
g-C_3N_4/MnO-5	0.90-37.56	3.49-52.91	19.73-9.53	10.79